



10<sup>th</sup> International Conference on Structural Dynamics, EURODYN 2017

# Fuzzy finite element model updating of a laboratory wind turbine blade for structural modification detection

Heather Turnbull\*, Piotr Omenzetter

*The Lloyd's Register Foundation Centre for Safety and Reliability Engineering, The University of Aberdeen, Aberdeen AB24 3UE, UK*

---

## Abstract

Wind turbine blades are a key structural component of the wind turbine and are crucial to efficient energy generation. The consequences of blade failure can be very expensive or even catastrophic and therefore a means of continuously monitoring the blades to determine their condition will provide substantial benefits. In this research, a novel application of Fuzzy Finite Element Model Updating (FFEMU) to wind turbine blades for their structural health assessment is demonstrated. Experimental frequencies obtained from modal analysis on a small-scale wind turbine blade were described by fuzzy numbers to model measurement uncertainty. Structural modification, intended to be in lieu of damage, was simulated experimentally in a non-destructive way through addition of a small mass to the blade trailing edge, inducing a structural change. A numerical model was constructed with the added mass parameters in several locations considered as updating parameters. Analyses were run with varying extents of the modification to obtain objective function values and fuzzy updated parameters were constructed that minimized the objective function. This methodology was able to successfully identify the location and extent of modification.

© 2017 The Authors. Published by Elsevier Ltd.

Peer-review under responsibility of the organizing committee of EURODYN 2017.

*Keywords:* Fuzzy finite element model updating; uncertainty quantification; structural health monitoring; damage severity assessment

---

## 1. Introduction

Costs associated with operation and maintenance (O&M) of wind turbines (WT) are approximately 20-30% of the lifecycle cost for onshore turbines and up to 30% of the already considerably higher lifecycle cost for offshore WTs [1]. To increase efficiency and cost effectiveness of WTs it is necessary to decrease these O&M costs whilst improving the reliability of the structures. In particular, wind turbine blades (WTB) are a key component of the WT with significant associated costs and downtime implications. The benefit of Structural Health Monitoring (SHM) techniques for early damage detection of WTBs will provide great benefit to WT operation.

Physics based SHM techniques like calibration of finite element models (FEM) by inverse techniques have developed significantly in recent years. Deterministic finite element model updating (FEMU) involves construction of an objective function, containing the variation between experimental and analytical modal parameters, which is minimised to determine a set of updated model parameters. This method does not account for uncertainties associated with the updated parameters arising from sources such as measurement noise and inaccurate FEMs. Probabilistic and non-probabilistic (fuzzy) uncertainty quantification methods can use uncertain measurement data and FEMs to propagate uncertainty into the updating parameters.

Probabilistic FEMU is dependent on assumptions regarding the random distribution of measured modal parameters to determine statistical indices of structural (updated) parameters. Damage identification using probabilistic updating was studied by Behmanesh and Moaveni [2] through experimentally adding mass to a footbridge and capturing vibration data in operational conditions. A numerical model was updated to successfully locate and predict the added mass. Fuzzy finite element model updating (FFEMU) was discussed by Erdogan and Bakir [3] to investigate the effect of measurement noise on measured modal parameters. Global optimization algorithms (GOAs) were utilised to determine the global optimum of the objective function at each fuzzy membership level with comparisons drawn about membership functions of fuzzy updated parameters and results obtained via MCS methods. FFEMU was further investigated by Liu and Duan [4] for a full-scale bridge structure. This work considered the uncertain structural parameters as fuzzy variables, which led to fuzzification of the objective function for updating. Approaches reported in both [3] and [4] involve model updating of structures with data containing reducible uncertainty.

This research is focused on non-probabilistic FFEMU methods which require no assumptions regarding the statistical distribution of uncertain variables. In contrast to probabilistic methods, FFEMU can handle more easily non-linear dependencies between modal parameters and structural parameters. In the present study, the FFEMU process is demonstrated for assessment of structural modification extent of a small scale WTB considering uncertainty propagation in updated parameters. Two experimental campaigns, in the baseline and altered states, were conducted to obtain the natural frequencies of the blade to be used as the target for updating studies. A numerical model was constructed with the added mass parameter of masses at specified locations considered to be updating parameters. Numerical analyses were run with varying extents of modification (mass change) to obtain the responses for varying modification extents. The objective function value for each combination was then calculated and fuzzy updated parameters which minimised the objective function at each fuzzy membership level were constructed.

## 2. Theory

### 2.1. Fuzzy sets and $\alpha$ -level technique

As the real-life situations entail fuzziness of variables such as those used in structural models, the fuzzy set method is a very powerful mechanism to quantify this uncertainty. In classical set theory, the statement about an object belonging to a particular set is described in binary terms, providing sharply defined boundaries. Fuzzy set theory, developed by Zadeh [5], on the other hand, assigns each object with a degree of membership within a particular set through prescription of a membership function. For a fuzzy set  $\tilde{A}$ , the membership function is represented by  $\mu_{\tilde{A}}(x)$  for all values of  $x$  in the domain  $X$ :

$$\tilde{A} = \{(x, \mu_{\tilde{A}}(x)) \mid (x \in X, \mu_{\tilde{A}}(x) \in [0,1])\} \quad (1)$$

A value of  $\mu_{\tilde{A}}(x)$  equal to one indicates that element  $x$  is undoubtedly a member of the set  $\tilde{A}$ , while a value of  $\mu_{\tilde{A}}(x)$  equal to zero indicates  $x$  is obviously not a member of set  $\tilde{A}$ . A value between these two extremes indicates a degree of belief in the variable belonging to the set. Fuzzy arithmetic often involves the implementation of the  $\alpha$ -level technique, dividing the membership function of fuzzy variables into multiple levels, enabling a deterministic interval to be obtained for each level. This technique to model vagueness and ambiguity is particularly useful in the context of structural engineering where imprecision is commonplace.

2.2. Fuzzy finite element model updating

A description of the FFEMU process adopted within this research can be seen in Figure 1. The objective functions detailed in section 2.3 will be used for updating at the individual  $\alpha$ -levels. The figure shows that the updating process is carried out at each of the  $m$   $\alpha$ -levels with the results of updating parameters at deterministic and fuzzy levels assembled to provide fuzzy updated parameters.



Figure 1 - Fuzzy finite element model updating process

2.3. Objective functions for fuzzy model updating

An objective function is used to minimise the deviation between experimental modal parameters and those predicted analytically. During the process of FFEMU, two objective functions are required, a deterministic function and a fuzzy objective function. The deterministic objective function used in this study, considering only frequencies, is:

$$\Pi = \sum_{i=1}^n \left[ (\lambda_i^a - \lambda_i^e) / \lambda_i^e \right]^2 \tag{2}$$

where  $\lambda$  represents eigenvalue (frequency), superscripts  $a$  and  $e$  refer to analytical and experimental values, respectively, and  $n$  is the number of frequencies considered. A fuzzy objective function is used to determine the interval updating parameter vector which minimises the deviation between experimental and analytical results [3]:

$$f(\theta^t) = \underline{\mathbf{r}}(\theta^t)^T \mathbf{W} \underline{\mathbf{r}}(\theta^t) + \bar{\mathbf{r}}(\theta^t)^T \mathbf{W} \bar{\mathbf{r}}(\theta^t), \quad \underline{\mathbf{r}}(\theta^t) = \left[ \underline{\lambda}_j^a(\theta^t) - \underline{\lambda}_j^e \right] / \underline{\lambda}_j^e, \quad \bar{\mathbf{r}}(\theta^t) = \left[ \bar{\lambda}_j^a(\theta^t) - \bar{\lambda}_j^e \right] / \bar{\lambda}_j^e \tag{3}$$

where  $\theta^t$  is the interval updating parameter vector,  $\underline{\lambda}_j^a(\theta^t)$  and  $\bar{\lambda}_j^a(\theta^t)$  are the lower and upper intervals of analytical eigenvalue, respectively, whilst  $\underline{\lambda}_j^e$  and  $\bar{\lambda}_j^e$  are the lower and upper intervals of experimental eigenvalues, respectively, and  $\mathbf{W}$  is the weighting matrix. Variables  $\underline{\mathbf{r}}$  and  $\bar{\mathbf{r}}$  are relative frequency errors.

3. Physical system and experiments

3.1. Experimental configuration

An experimental campaign on a small scale WTB was carried out to determine the modal parameters of the healthy (baseline state) WTB in laboratory conditions for use in model calibration studies. The blade was from a utility scale Fortis WT with 5 kW power output and 5 m rotor diameter. The blade is manufactured through pultrusion of glass-fibre reinforced epoxy composite creating a solid cross section with a E387 profile and height of 2.36 m. The total mass and mass density of the specimen were estimated from measurements to be approximately 7.11 kg and 2,300 kg/m<sup>3</sup>, respectively. A fixed-free configuration, with the blade clamped at the root to a heavy steel base placed on a heavy concrete floor, was chosen to simulate the support of an in-service WTB and minimise the influence of uncontrolled ambient excitations. The blade was configured vertically to save lab space.

Experimental modal analysis was conducted to determine the dynamic modal parameters of the structure in its baseline state. Using a roving hammer methodology, the structure was impacted with a Brüel & Kjær 8206 impact hammer with sensitivity of 1.14 mV/N, effective mass of 0.1 kg and maximum force of 4,448 N in 26 locations as defined in Figure 2. To mitigate against any potential poor impacts, each location was struck ten times with the results averaged. To excite the structure in the desired frequency range, a soft polyurethane tip was used, enabling the structure to be excited in a frequency range of 0-550 Hz. To measure the response acceleration of the blade, two

accelerometers were attached using wax to the leading and trailing edge corners of the blade as demonstrated in Figure 2. Force and acceleration readings were taken at a sampling rate of 2,048 Hz with a measurement time of 80 seconds for each impact. Although a single accelerometer would have been sufficient for the purpose, it was decided to use two for comparison purposes and beneficial data redundancy. Two miniature piezoelectric accelerometers model Metra KS94B-100 with an individual weight of 3.2 g, voltage sensitivity of 98.95 mV/g and an operational frequency range of 0.5–28 kHz were used. The force and acceleration signals were digitized with a National Instruments (NI) NI-9234 data acquisition card connected to a NI cDAQ-9174 chassis and laptop. NI LabView software was used for signal processing.

### 3.2. Experimental modal analysis results in baseline state

Dynamic characteristics of the blade were identified using two system identification (S-Id) methods to provide confidence in the results obtained. Accelerance frequency response functions (FRF) enable the analyst to construct a mathematical model which describes the dynamic behaviour of the structure. The average magnitude FRF (AMFRF), similar to the averaged normalised power spectral density [6], was used for a quick modal frequency identification using peak picking. The AMFRF is defined as:

$$AMFRF_i(f) = \sum_{j=1}^{N_j} |H_{ij}(f)| / N_j \quad (4)$$

where  $N_j$  is the number of excitation locations and  $|H_{ij}(f)|$  is the averaged magnitude FRF estimated from numerous measurements at various excitation locations. Averaging of FRFs in this manner results in a loss of information regarding the local properties of the structure, however, it is suitable for determining the global properties of the structure. The AMFRF of measurements obtained can be seen in red in Figure 3. The peaks shown in the FRF plot indicate the natural frequencies. The first 8 natural frequencies are provided in Table 1, with the low first natural frequency indicative of the high flexibility of the WTB. To provide increased confidence in the results obtained, a subspace identification (SSI) method as described by [7] was run ten times with the results averaged, the outcomes of which can also be seen in Table 1. The standard deviations associated with each methodology were found to be very low, and near perfect agreement observed between peak picking and SSI, therefore these results are deemed acceptable for further investigations.

### 3.3. Experimental modal analysis results in altered state

According to visual inspections of ninety-nine 100 kW and 300 kW WTs by Ataya and Ahmed [8] damage in the form of cracking is most likely to occur at around 73% length on the blade trailing edge. Therefore, to simulate damage experimental modification was located at the WTBs trailing edge at 70% blade length. A thin metal plate was glued to the structure which facilitated the attachment of a 75x50x20 mm ferrite magnet. The weight of this assembly was measured to be 0.405 kg (5.7% total blade weight). Addition of a small mass to the structure will induce a structural change that can be studied in lieu of actual damage whilst preventing permanent damage to the structure.

A comparison between the AMFRF obtained from both baseline and altered state can be seen in Figure 3. Obtained through AMFRF peak picking, the natural frequencies of the structure in its altered state can be seen in Table 2 with percentage reduction compared to the baseline state highlighted. The effect of added mass varies significantly between 0.4% and 11.8%.

### 3.4. Fuzzification of experimental results

To create fuzzy experimental results, the AMFRF values obtained in Table 1 were considered to be deterministic values with the membership value of one for sub-level  $\alpha=1$ . To account for uncertainty in measurement and system identification, the experimental data were modelled as symmetric fuzzy numbers with triangular membership functions.

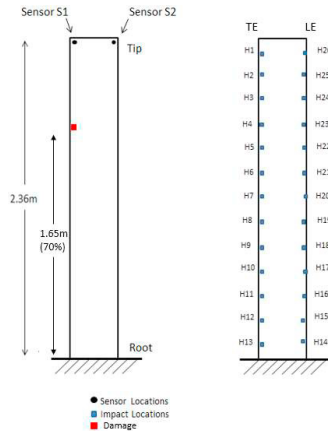


Figure 2 - Hammer impact, sensor and damage locations

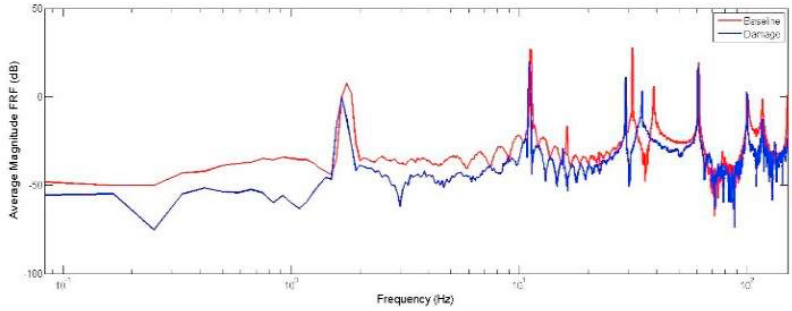


Figure 3 - AMFRF comparison between baseline (red) and altered (blue) states

Table 1 – Experimental natural frequencies for baseline state

Mode no.	AMFRF frequency (Hz)	Standard deviation (Hz)	SSI frequency (Hz)	Standard deviation (Hz)
1	1.75	0.00	1.75	0.00
2	11.2	0.00	11.2	0.00
3	31.3	0.00	31.3	0.00
4	38.8	0.00	38.8	0.01
5	61.3	0.00	61.3	0.00
6	100.4	0.01	100.5	0.00
7	116.3	0.01	116.4	0.01
8	149.4	0.01	149.3	0.00

Table 2 - Comparison of experimental natural frequencies between baseline and altered state

Mode no.	Baseline state frequency (Hz)	Altered state frequency (Hz)	Relative error (%)
1	1.75	1.67	-4.8
2	11.2	11.1	-0.7
3	31.3	29.3	-6.6
4	38.8	34.6	-10.9
5	61.3	60.7	-1.0
6	100.4	99.4	-1.0
7	116.3	115.8	-0.4
8	149.4	131.8	-11.8

Intervals at level  $\alpha=0$  were chosen based on typical measurement error variance and assumed modelling error variance. The measurement error at each  $\alpha$ -level was defined as [9]:

$$\Delta_{\alpha,j}^D = (1-\alpha)z\sigma_j \tag{5}$$

where  $\sigma_j$  estimates the standard deviation of measurement error associated with the  $j$ -th eigenvalue and  $z$  incorporates a confidence interval of errors into the  $\alpha$ -level. The modelling error at each  $\alpha$ -level was defined as [9]:

$$\Delta_{\alpha,j}^G = (1-\alpha)z\varepsilon_j\lambda_{ej} \tag{6}$$

where  $\varepsilon_j$  determines the magnitude of the modelling error. For this investigation,  $\sigma_j=0.01$  Hz and  $\varepsilon_j=0.01$  represents an assumed 1% modelling error and  $z$  is a function of the normal inverse cumulative distribution function. With a 99% confidence interval chosen the corresponding value was  $z=2.58$ . The interval bounds were then linearly interpolated to obtain the upper and lower bounds of measured data at each  $\alpha$ -level as [9]:

$$\left[ \tilde{\lambda}_j^e \right]_{\alpha} = \left[ \lambda_j^e - \Delta_{\alpha,j}^D - \Delta_{\alpha,j}^G, \lambda_j^e + \Delta_{\alpha,j}^D + \Delta_{\alpha,j}^G \right] \tag{7}$$

## 4. Numerical model

### 4.1. Numerical Model updating – baseline state

A numerical model of the experimental test specimen defined in section 3.1 was created using ABAQUS software. The model consists of 9,828 nodes and 1,775 solid elements. Encastre boundary conditions are placed upon the bottom of the blade to simulate the clamped configuration within laboratory experiments. With limited material specifications available from the manufacturer of the glass-fibre reinforced epoxy composite blade, an initial estimate of material properties was required. Material properties of an epoxy composite with unidirectional glass fibre reinforcement, known as E-glass 21xK43 Gevetex, defined by Soden et al. [10] were utilised. To update the FEM, the longitudinal modulus,  $E_1$ , and in-plane shear modulus,  $G_{12}$ , were chosen as updating parameters.

The first stage of fuzzy updating involves deterministic updating at  $\alpha$ -level  $\alpha=1$  which includes minimisation of the deterministic objective function in equation (2) containing the difference between analytical and experimental eigenvalues using the particle swarm optimisation (PSO) algorithm [11]. A population of 10 particles were generated and the maximum number of iterations specified as 50. A methodology developed by Clerc and Kennedy [12] suggests PSO parameters such as the inertial weight equal to 0.73 and the personal/social acceleration coefficients are both equal to 1.45. At each iteration of the PSO algorithm, updated values were obtained using the ABAQUS2Matlab toolbox [13]. The output of this stage is the determination of a vector of updating parameters with eigenvalues corresponding to the values specified in Table 1. In subsequent stages, fuzzy experimental results were used to conduct interval model updating at each individual  $\alpha$ -level. This was achieved through minimization of a fuzzy objective function in equation (3) containing the difference between analytical and experimental frequencies at the lower and upper bounds respectively using the same PSO algorithm. The output of this stage was an interval vector containing the lower and upper values of the updated parameters. The final fuzzy parameters were obtained by combining the deterministic and interval valued updating parameters at each  $\alpha$ -level. The minimum value was found to occur when  $E_1$  and  $G_{12}$  were 62.15 GPa and 8.33 GPa respectively. The updated deterministic material properties of the baseline model can be seen in Table 3.

A comparison between the initially assumed material properties from [10] and the deterministic updated values can be seen in Table 3. Material properties estimated for the deterministic case provide the frequency values shown in Table 4 with largest variation shown to decrease significantly through updating to be around 2.46% for the first mode of vibration. Deterministically updated values of material properties in Table 3 were used in modification extent assessment discussed in section 5. Over estimation of the first bending mode frequency may be due to the modelling inaccuracies resulting from idealizing the encastre boundary conditions specified; further study will involve modelling the boundary conditions as springs and including these as updating parameters during model calibration.

As discussed, this process was repeated using the fuzzy experimental analysis results calculated in Section 0 to obtain the fuzzy updating parameters shown in Figure 4. These parameters were obtained by calculation of interval updating parameter vector at each subsequent  $\alpha$ -level; deterministic and interval updating parameter vectors were then

Table 3 - Initial [10] and updated material properties for baseline state

Material property	Initial model	Updated model
Longitudinal modulus, $E_1$ (GPa)	53.48	62.15
Transverse modulus, $E_2$ (GPa)	17.70	17.70
In-plane shear modulus, $G_{12}$ (GPa)	5.83	8.33
Major Poisson's ratio, $\nu_{12}$	0.278	0.278
Through thickness Poisson's ratio, $\nu_{23}$	0.400	0.400

Table 4 - Frequency comparison between experimental and initial and updated models for baseline state

Mode no.	1	2	3	4	5	6	7	8
Experimental (Hz)	1.75	11.2	31.3	38.8	61.3	100.5	116.4	149.3
Initial model (Hz)	1.66	10.4	29.0	32.5	56.6	92.9	99.7	138.0
Updated model (Hz)	1.79	11.2	31.3	38.8	61.2	100.5	117.2	149.3
Initial model error (%)	-5.00	-7.1	-49.3	-25.2	-47.0	-43.6	-20.1	-36.6
Updated model error (%)	2.46	0.1	0.0	0.0	-0.2	0.0	0.7	0.0

assembled to produce the fuzzy variables shown. Comparisons between the frequency values obtained for both fuzzy experimental and updated fuzzy model, Figure 5, show close correlation of frequencies.

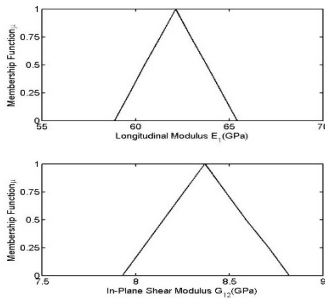


Figure 4 – Fuzzy updated parameters for baseline state

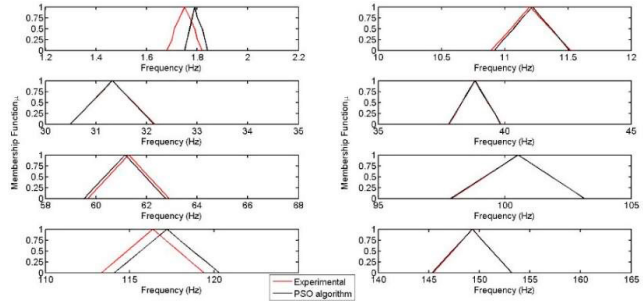


Figure 5 - Frequency comparison between fuzzy experimental results and fuzzy updated parameters in baseline state

### 5. Structural modification identification

#### 5.1. Simulating the effects of structural modification

During this investigation, a singular modification location was considered with natural frequency values used as targets during updating. The updated analytical model in Section 4.1 was developed to identify the location and magnitude of experimental modification, physically simulated through addition of a mass at 70% length on the blades TE. To replicate this in the numerical model four masses, with variable magnitude, were modelled at the defined points highlighted in Figure 6. The mass of individual structural alterations, labelled  $M_n$  with  $n$  denoting the mass number, were considered as updating parameters. Insight into the placement of experimental mass led to the numerical masses being concentrated more heavily in the 50-75% region of the blade.

#### 5.2. Results of updating with structural alteration

For the damage identification problem, PSO was initialized with the same parameters as in Section 4.1. The process of deterministic updating at  $\alpha=1$  was carried out through construction and minimisation of an objective function, of the form equation (2), using the PSO algorithm described. To obtain the inputs to the PSO algorithm ABAQUS2Matlab toolbox [13] was utilised. The deterministic updated parameters obtained can be seen in Table 5 and Figure 7, highlighting the accuracy with which PSO is able to identify the location and magnitude of damage. The methodology predicted a mass magnitude of 0.393 kg at  $M_3$  which is within 3% of the experimental value. A less significant mass magnitude was also predicted upon  $M_2$  of 0.066 kg which could be a result of baseline updating and will be the focus of future research.

Using experimental fuzzy numbers determined from the altered state AMFRFs, interval updated parameter vectors were calculated at each  $\alpha$ -level through minimizing an equation of the form (3) and then assembled with the deterministic value to produce the results shown in Figure 7. The results show sections 1 and 4 to have the smallest uncertainty with no structural modification present in these sections. Modification in section 3 is highlighted with the associated uncertainty revealed to vary within  $0.321 < M_3 < 0.422$  kg. The updated deterministic frequency values can be seen in Figure 8, highlighting coherence between results. The greatest degree of variation was observed in modes 1, 5 and 7 and is thought to be attributed to the discrepancies encountered in initially updating the baseline model, Figure 5.

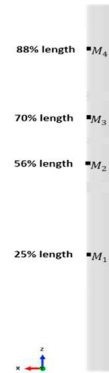


Figure 6 - Blade FEM with added numerical masses highlighted

Table 5 - Deterministic damage identification comparison between experimental and PSO updated

Added Mass	Experimental (kg)	PSO-Updated (kg)
M1	0.000	0.000
M2	0.000	0.066
M3	0.405	0.393
M4	0.000	0.000

## 6. Conclusions

In this paper, the theory behind FFEMU was introduced and applied to update small-scale WTB FEM using experimentally determined natural frequencies obtained through impact hammer testing in both the baseline and altered states. Fuzzy membership functions of these experimental results were constructed and the fuzzy sub-level technique was initially used to update the baseline model of the blade, and then to detect the extent and location of experimental modification simulated (added mass). This enabled the construction of fuzzy updating parameters, both for the baseline state and for the altered state. The demonstrated methodology successfully identified the location and amount of an experimental mass located at 70% length of the blade.

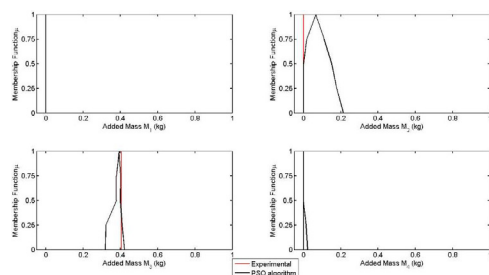


Figure 7 -Fuzzy updated parameters in altered state

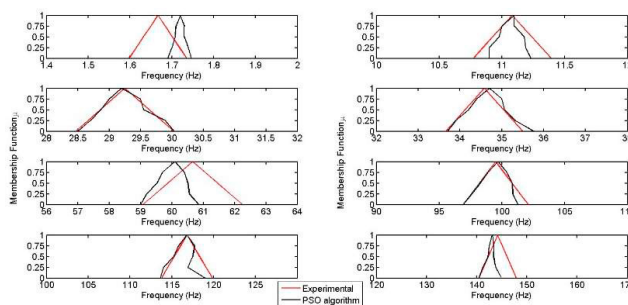


Figure 8 - Frequency comparison between fuzzy experimental results and fuzzy updated parameters in altered state

## Acknowledgment

Heather Turnbull's PhD study within the Lloyd's Register Foundation Centre for Safety and Reliability Engineering at the University of Aberdeen is supported by Lloyd's Register Foundation. The Foundation helps to protect life and property by supporting engineering-related education, public engagement and the application of research.

## References

- [1] Fischer, K., Besnard, F. and Bertling, L., (2012). Reliability-centered maintenance for wind turbines based on statistical analysis and practical experience, *Energy Conversion, IEEE Transactions On*, 27 (1), pp.184-195.
- [2] Behmanesh, I. and Moaveni, B., (2016). Accounting for environmental variability, modeling errors, and parameter estimation uncertainties in structural identification, *Journal of Sound and Vibration*, 374 pp.92-110.
- [3] Erdogan, Y.S. and Bakir, P.G., (2013). Inverse propagation of uncertainties in finite element model updating through use of fuzzy arithmetic, *Engineering Applications of Artificial Intelligence*, 26 (1), pp.357-367.
- [4] Liu, Y. and Duan, Z., (2012). Fuzzy finite element model updating of bridges by considering the uncertainty of the measured modal parameters, *Science China Technological Sciences*, 55 (11), pp.3109-3117.
- [5] Zadeh, L.A., (1965). Fuzzy sets, *Information and Control*, 8 (3), pp.338-353.
- [6] Felber, A.J. and Ventura, C.E., (1996). Frequency domain analysis of the ambient vibration data of the Queensborough bridge main span, *Proceedings of 14th International Modal Analysis Conference (IMAC)*, Dearborn, pp. 459-465.
- [7] Overschee, P.V. and De Moor, B., (1996). *Subspace Identification for Linear Systems*. Massachusetts, US: Kluwer Academic Publishers.
- [8] Ataya, S. and Ahmed, M.M.Z., (2013). Damages of wind turbine blade Trailing edge: forms, location, and root causes, *Engineering Failure Analysis*, 35 pp.480-488.
- [9] Simoen, E., De Roeck, G. and Lombaert, G., (2015). Dealing with uncertainty in model updating for damage assessment: A review, *Mechanical Systems and Signal Processing*, 56 pp.123-149.
- [10] Soden, P.D., Hinton, M.J. and Kaddour, A.S., (1998). Lamina properties, lay-up configurations and loading conditions for a range of fibre-reinforced composite laminates, *Composites Science and Technology*, 58 (7), pp.1011-1022.
- [11] Kennedy, J. and Eberhart, R., (1995). Particle swarm optimization, pp. 1942-1948.
- [12] M. Clerc and J. Kennedy, (2002). The particle swarm - explosion, stability, and convergence in a multidimensional complex space, *IEEE Transactions on Evolutionary Computation*, 6 (1), pp.58-73.
- [13] Papazaferiopoulos, G., Muñiz-Calvente, M. and Martínez-Pañeda, E., (2017). Abaqus2Matlab: a suitable tool for finite element post-processing. *Advances in Engineering Software* (2017), Available at: <http://www.abaqus2matlab.com/>